

## Optical observations of RS Oph after its 2021 outburst

M. Tomova<sup>1</sup>, K. Stoyanov<sup>1</sup>, Y. Nikolov<sup>1</sup> and P. Kaygorodov<sup>2</sup>

<sup>1</sup> *Institute of Astronomy and NAO, Bulgarian Academy of Sciences,  
72 Tsarigradsko Chausse Blvd., BG-1784 Sofia, Bulgaria*

<sup>2</sup> *Institute of Astronomy of the Russian Academy of Sciences, 48 Pyatnitskaya  
Str., 119017 Moscow, Russia*

Received: November 2, 2023; Accepted: January 11, 2024

**Abstract.** RS Oph is a recurrent symbiotic novae which underwent its last optical eruption in August 2021. The early H $\alpha$  spectroscopy of the system (at days 11–15 of the outburst) reveals satellite line components at the velocity position of about  $\pm 2400 \text{ km s}^{-1}$  which are an indication of bipolar collimated outflow. We derived some parameters of the outflows and system's components and their evolution during our observation.

**Key words:** binaries: symbiotic – stars: mass-loss – stars: individual: RS Oph

### 1. Introduction

RS Oph consists of a red giant and a massive white dwarf with a heavy mass loss during activity. Its last 2021 outburst began on August 8.93<sup>1</sup> and was observed over the whole electromagnetic domain. Here we report high-resolution H $\alpha$  spectroscopy of the system, obtained at days 11–15 (August, 19–23) of the outburst with the Coudé spectrograph of the 2m RCC telescope at Rozhen NAO, Bulgaria. We present low-resolution observations (the resolving power is  $R \sim 1100$ ) secured with the 2-Channel-Focal-Reducer Rozhen, attached to the Cassegrain focus of the 2m RCC telescope as well.

### 2. Spectral Energy Distribution (SED)

To examine the outflow structure of the outbursting compact object, we built the SED of the system for the first and last day of the observations. We used average  $U$ ,  $B$ ,  $V$ ,  $R_C$ , and  $I_C$  photometric estimates from the light curves of the AAVSO database<sup>2</sup> taken during our observations from August 19 to 23. The approximation of the  $UBVR_CI_C$  fluxes showed that for this period  $T_{\text{eff}}$  of the pseudophotosphere and  $T_e$  of the nebula have not changed:  $T_{\text{eff}} = 15\,000 \pm 1\,000 \text{ K}$

---

<sup>1</sup>Geary, K., 2021, AAVSO Alert Notice 752 (20210809)

<sup>2</sup>International Database contributed by observers worldwide.

and  $T_e = 17\,000 \pm 3\,000$  K. We obtained  $R_{\text{eff}} = (13.3 \pm 2.0)(d/1.6\text{kpc}) R_{\odot}$  and  $EM = (9.50 \pm 0.59) 10^{61} (d/1.6\text{kpc})^2 \text{cm}^{-3}$  for August 19 and  $R_{\text{eff}} = (10.3 \pm 1.6)(d/1.6\text{kpc}) R_{\odot}$  and  $EM = (5.60 \pm 0.35) 10^{61} (d/1.6\text{kpc})^2 \text{cm}^{-3}$  for August 23. The SED is presented in Fig. 1 (Tomov et al., 2023).

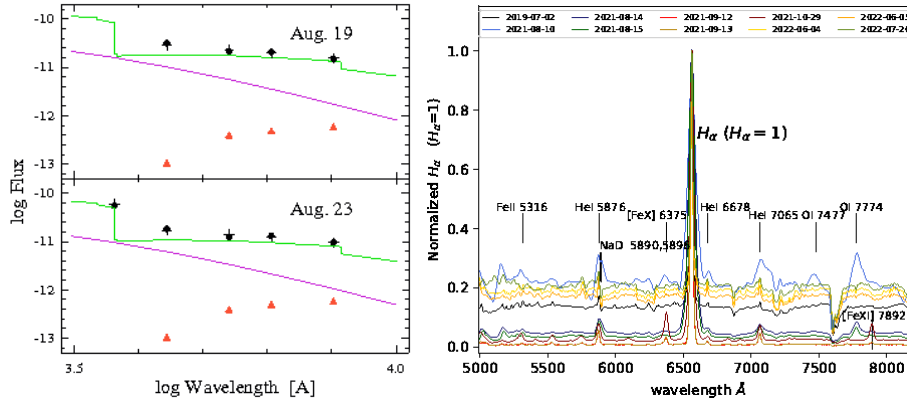


**Figure 1.** *Left panel:* SED for days 11 and 15 (see Tomov et al., 2023). *Right panel:* Spectral evolution based on low-resolution spectra (see Nikolov et al., 2023).

### 3. $H\alpha$ profile, spectral evolution and mass-loss rate

Our spectral observations reveal a typical behaviour of a nova with a complex structure dominated by broad Balmer, He, O and Fe lines with some P Cyg profiles, evolved towards a supersoft source phase (see Fig. 1). The most prominent feature on the spectra is the  $H\alpha$  emission line. A P Cyg profile with velocity up to  $\sim -4260 \text{ km s}^{-1}$  (Nikolov, 2023) is detected on day 2 (Aug. 10).

The complex structure of  $H\alpha$  line is better seen in our high-resolution spectra, obtained at days 11–15 of the outburst (Tomov et al., 2023). The  $H\alpha$  profile has strongly changed – the very sharp emission and absorption spikes, which were observed at day 2.3 (Munari et al., 2022) on top of the much wider and stronger emission line, were very weak. The very intensive broad component had an appreciable asymmetry and very broad low-intensity wings reaching  $\pm 3500 \text{ km s}^{-1}$  (Fig. 2). We assume this velocity to be related to nebular material ejected by the outbursting component.  $H\alpha$  had very weak satellite components at a velocity position of about  $\pm 2400 \text{ km s}^{-1}$  as well. We suppose that the satellite components are an indication of bipolar outflow from the outbursting component as during the 2006 eruption. It is worth noting that satellite components were also present in 2006 (Skopal et al., 2008) and they were much more intense relative to the central emission of the line than during the 2021 eruption. To obtain the parameters of the stellar wind and bipolar outflow, we analysed the  $H\alpha$  profile by means of approximation with different functions, which are

shown in Fig. 2. The parameters of the satellite components determined by this approximation are listed in Tab. 1 (Tomov et al., 2023).

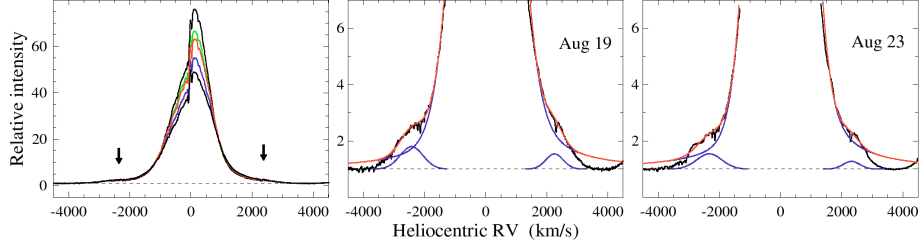


**Figure 2.** H $\alpha$  line. The spectrum of lowest intensity relates to August 19.

**Table 1.** Parameters of the satellite components. The flux is in units of  $10^{-10}$  erg cm $^{-2}$  s $^{-1}$ , velocity and FWHM in km s $^{-1}$ , linear angle  $\theta$  in deg, and mass-loss rate in  $10^{-6}(\text{d}/1.6\text{kpc})^{3/2} M_{\odot} \text{yr}^{-1}$ .

Date	Blue					Red				
	$F$	FWHM	$v/\cos i$	$\theta$	$\dot{M}$	$F$	FWHM	$v/\cos i$	$\theta$	$\dot{M}$
Aug 19	3.320	880	3780	35.6	1.2	1.706	670	3500	29.0	0.6
Aug 20	2.846	1000	3720	41.2	1.2	1.608	850	3460	37.5	0.8
Aug 21	2.699	1040	3640	43.8	1.2	1.352	780	3540	33.5	0.6
Aug 22	2.243	1030	3620	43.7	1.0	1.145	840	3500	36.7	0.6
Aug 23	1.559	970	3620	40.9	0.8	0.519	640	3610	26.7	0.3

## 4. Conclusions

We analysed the H $\alpha$  profile with the aim being to study the structure of the outflowing material. We observed a disc-shaped warm shell occulting the central hot object and bipolar outflow. We find that during the 2021 eruption, about 30%–50% of the nebular emission belongs to the high-velocity wind, the H $\alpha$  luminosity of which was less than  $2700 L_{\odot}$ . The mass-loss rate of the outbursting object through its wind is much greater than through its streams. The total rate (from wind + streams) was less than  $(4 - 5) 10^{-5} (\text{d}/1.6\text{kpc})^{3/2} M_{\odot} \text{yr}^{-1}$ .

**Acknowledgements.** This work was supported by Bulgarian National Science Fund under grant KP-06-Russia/2-2020 and RFBR grant 20-52-18015.

## References

- Munari, U., Giroletti, M., Marcote, B., O'Brien, T.J., Veres, P., Yang, J., Williams, D. R. A., Woudt, P.: 2022, *A&A*, **666**, L6
- Nikolov, Y., Luna, G.J.M., Stoyanov, K.A., et al.: 2023, *A&A*, **679**, A150
- Skopal, A., Pribulla, T., Buil, Ch., Vittone, A., Errico, L.: 2008, in *ASP Conf. Ser.*, Vol. **401**, 227
- Tomov, N.A., Tomova, M.T., Stoyanov, K.A., et al.: 2023, *A&A*, **671**, A49